A three-dimensional potential energy surface for dissociative adsorption and associative desorption at metal electrodes

A three-dimensional potential energy surface for dissociative adsorption and associative desorption at metal electrodes

Marc T. M. Koper
Schuit Institute of Catalysis, Laboratory of Inorganic Chemistry and Catalysis, Eindhoven University of Technology, 5600 MB Eindhoven, The Netherlands

Gregory A. Voth
Department of Chemistry and Henry Eyring Center for Theoretical Chemistry, University of Utah, Salt Lake City, Utah 84112-0850

(Received 27 February 1998; accepted 28 April 1998)

A simple model is constructed to calculate the potential energy surface of dissociative adsorption and associative desorption reactions at the metal/solution interface. The model is based on an extension of the Anderson–Newns Hamiltonian and has three reaction coordinates; the bond length or the distance between the fragments, the distance from the surface, and the generalized solvent coordinate familiar from the classical theory of electron-transfer reactions. The properties of the three-dimensional potential energy surfaces are studied and the activation energy for dissociative adsorption is calculated as a function of the applied potential and the metal work function. In the observed trends, the absorption energy and hence the electrosorption valency of the fragments play an important role. For certain ''extreme'' values of the bonding or antibonding energy levels, molecular ions may become metastable and affect the reaction mechanism. © *1998 American Institute of Physics.* [S0021-9606(98)70529-X]

I. INTRODUCTION

Undoubtedly the key event in heterogeneous catalytic reactions is the step in which a molecule dissociatively adsorbs, or adsorbed fragments combine, to form new chemical entities. The modeling of such reactions is the central issue of theoretical heterogeneous catalysis. Theoretical approaches to chemisorption, dissociative chemisorption, and associative desorption may involve various levels of sophistication.[1] The quantum chemistry of such systems may be treated by model Hamiltonians, by semiempirical methods such as the extended Hückel method, or by *ab initio* methods based on self-consistent-field Hartree–Fock theory or density functional theory. The semiempirical and *ab initio* approaches usually involve cluster models of the metal surface, and although these cluster models have their limitations, with the present level of computational capabilities quite satisfactory and insightful results are attainable for simple reactions at the single-crystal/UHV interface.[1]

The situation is much more complicated for catalytic reactions at metal/liquid interfaces as two formidable problems arise which are not yet satisfactorily treatable by cluster models. The first is the presence of the solvent and the electrolyte ions which are definitely going to have an influence on the rate and the selectivity of many heterogeneously electrocatalyzed reactions. The second problem is the presence of an electric field due to an excess charge on either side of the interface. This basically reduces to the problem of how to include a continuously adjustable electrode potential in a cluster model of the metal. So far only the latter problem has been tackled in the context of cluster models by Anderson[2] in his atom superposition and electron delocalization molecular orbital (ASED-MO) theory, a semiempirical method.[3] By parameterizing the ionization potentials of the atoms constituting the metal cluster, this method allows for a continuous shift of the electronic bands and the Fermi level of the metal. However, in Anderson's method the electrode surface remains uncharged and no electric field exists in the double layer.

Recently, progress has been made in the modeling of various classes of electrochemical reactions by model Hamiltonians. Schmickler[4,5] was the first to extend a well-known model Hamiltonian from surface physics, the so-called Anderson–Newns Hamiltonian,[6] to the electrochemical interface by including the coupling with the polar solvent. Several extensions of Schmickler's model have been suggested since, including treatments of outer- and inner-sphere electron transfer at metal[7–13] and semiconductor electrodes,[14,15] proton transfer,[16] ion transfer[17–20] and concerted bond breaking electron transfer reactions at metal electrodes.[21] Although these approaches will never give information as detailed as ''first-principles'' simulations or quantum-chemical calculations, they are very useful as conceptualizations of certain classes of electrode reactions. Furthermore, owing to their relative simplicity, they more readily give insight into the potential dependence of the reaction rate, clearly a central issue in electrode kinetics.

In this paper a new extension of Schmickler's Anderson–Newns Hamiltonian is suggested which allows the calculation of the potential energy surface (PES) of dissociative adsorption and associative desorption at a metal electrode. This seems to be the first microscopic model of a truly electrocatalytic reaction in which bonds are broken or formed. The dimension of the PES is higher than that of any previous model of electrochemical reactions, as there are

three reaction coordinates proper to this process; the distance of the center of mass of the molecule or the fragments from the electrode, the bond length of the bond being broken or the distance between the two fragments, and the polarization state of the solvent or total charge of the reactive complex. The latter coordinate, the well-known solvent coordinate from the Marcus[22] and Levich–Dogonadze[23] theories, is unique to condensed-phase charge transfer reactions and has no counterpart in dissociative adsorption reactions at the metal/gas interface.

A few words on the organization of the paper. In Sec. II, we give the Hamiltonian describing the system, which consists in fact of two Hamiltonians, one describing the molecule and one describing the fragments. The two adiabatic ground-state potential energy surfaces which follow from both Hamiltonians are calculated, and we then calculate the total potential energy surface by simply ''mixing'' the potential energy surfaces of the two subsystems. Our model treats both oxidative and reductive dissociative adsorption. In Sec. III the properties of the resulting potential energy surface are studied, deriving the typical reaction path, identifying the rate-determining step(s), and calculating the activation energy of the bond breaking step and its dependence on parameters such as potential and metal work function. A short summary of our results is given in Sec. IV.

II. THE HAMILTONIAN AND THE GROUND STATE PES

Our aim in this paper is to calculate the PES for the following electrode reactions:

$$X_2 + 2e^- \rightleftharpoons 2X^- \tag{2.1}$$

and

$$Y_2 \rightleftharpoons 2Y^+ + 2e^-, \tag{2.2}$$

where we will refer to X_2 (Y_2) as the molecule and X^- (Y^+) as the fragment(s). In principle, the fragment can be any chemical entity. However, we concentrate more specifically on reaction (2.1) with X being a halide, e.g.,

$$Cl_2 + 2e^- \rightleftharpoons 2Cl^-. \tag{2.3}$$

A typical example of reaction (2.2) would be the H_2 oxidation. However, our model is certainly too crude to describe hydrogen, as this would have to include a much more accurate description of the proton–solvent interaction than the simple purely electrostatic model considered below.

In the classical electrochemical literature,[24,25] the above reactions are usually believed to follow either a so-called Tafel–Volmer mechanism,

$$\begin{aligned} &X_2 \rightleftharpoons 2X_{\text{ads}}, \\ &X_{\text{ads}} + e^- \rightleftharpoons X^-, \end{aligned} \tag{2.4}$$

or a so-called Heyrovsky–Volmer mechanism,

$$\begin{aligned} &X_2 + e^- \rightleftharpoons X_{\text{ads}} + X^-, \\ &X_{\text{ads}} + e^- \rightleftharpoons X^-. \end{aligned} \tag{2.5}$$

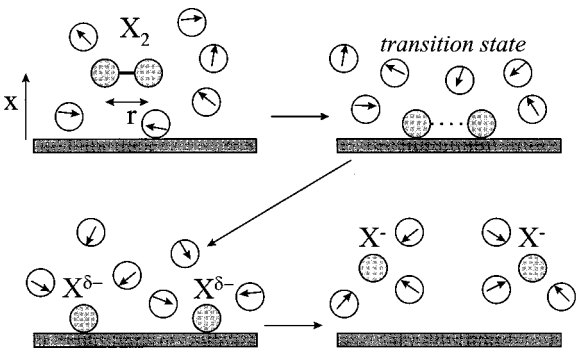

FIG. 1. A pictorial view of the Tafel–Volmer mechanism.

[Surface chemists would refer to (2.4) as a Langmuir–Hinshelwood mechanism and to (2.5) as an Eley–Rideal mechanism.[26]] The theory to be described below will give a PES of the Tafel–Volmer mechanism.

Before we plunge into the equations, it is good to have a more pictorial and intuitive view of the physical events we are assuming to take place during the process. This qualitative description will sometimes anticipate the results of the quantitative modeling, but will allow us to introduce the three reaction coordinates that are needed to fully describe the system.

Considering the reductive dissociation (2.1), there is first the molecule approaching the surface along the distance coordinate x [Fig. 1(a)]. In our model, x describes the distance of the center of mass of the molecule from the surface. Throughout this paper, we consider the molecule in a position parallel to a featureless surface; perpendicular rotations are not taken into account. The molecule is attracted to the surface by van der Waals forces, and, when it gets close to the surface, by sharing electrons with the metal substrate in surface bonds. Part of the electronic attraction may be due to the donation of electrons to the antibonding orbital of the X_2 molecule, depending on how the energy of this antibonding orbital lies with respect to the Fermi level of the metal. The energy level of the antibonding orbital lowers as the molecule approaches the surface due to the image interaction. However, the backdonation of metal electrons to the antibonding orbital weakens the $X-X$ bond and the bond stretches along the bond coordinate r. At some critical point in phase space [Fig. 1(b), the transition state], it becomes favorable for the molecule to break up into two adsorbed fragments [Fig. 1(c)], r now describing the distance between the two fragments. The calculation of when this exactly occurs is the main objective of this paper. In a final step, the fragments desorb from the electrode surface and wander off into the solution [Fig. 1(d)]. During all these events, we will assume that the total charge distribution on the reactive system changes gradually and adiabatically. It is important to realize that there exists no single step in which exactly one entire electron is being exchanged with the electrode. This gradual ''charging'' of the reactive complex will involve a reorganization of the surrounding solvent and will therefore influence the total potential energy of the system. This solvent reorganization is the third reaction coordinate, and we will follow ideas from the Marcus[22]–Hush[27] theory by as-

suming that this collective solvent coordinate can be conveniently expressed by the total charge q. We note that the concept of a collective solvent coordinate implies that it is, strictly speaking, more accurate to speak of a free energy surface than a potential energy surface, but we will use the term potential energy surface throughout.

The picture for Y_2 dissociation is very similar, the main difference being that instead of the antibonding orbital we have to specify the bonding orbital which is able to donate electrons to the electrode and thereby weakening the $Y-Y$ bond. This last point is important as it means that, in this paper, we will assume that in reaction (2.2) there is no backdonation of metal electrons to the antibonding orbital of the Y_2 molecule. It is rather the donation of bonding electrons to the metal which is driving the breaking of the bond. We adopt this picture because we want our model for reaction (2.2) to be the ''mirror image'' of our model for reaction (2.1).

A. X_2 adsorption

We first describe the interaction of the X_2 molecule with the surface. We will consider only the electronic interaction of the antibonding LUMO energy level ϵ_a with the metal electronic levels. This is sufficient to describe the bond breaking process, although for a more accurate description of the adsorption process the interaction with the molecule's HOMO orbital will also be important.[28] This interaction will be included in a simplified way, as explained below. The Hamiltonian employed is equivalent to a Hamiltonian recently suggested to describe concerted bond breaking and electron transfer.[21] That model was studied mainly in the limit of weak electronic coupling, to model the reductive cleavage of molecules located in the outer Helmholtz plane, i.e., not adsorbed onto the metal surface. Such reactions have been studied in great detail by Savéant and co-workers.[29] It was noted in our previous paper that for stronger electronic coupling, the model was capable of describing the phenomenon of backdonation mentioned in the previous section. It is this feature of the model that will be exploited here. Backdonation is also held responsible for the potential-dependent IR stretch frequencies of electrochemically adsorbed diatomics such as NO and CO; in fact, to explain this phenomenon, a model quite similar to the one presented below was considered by Holloway and Nørskov.[30]

The Hamiltonian describing the X_2 interaction with the metal consists of three parts,

$$H=H_{\mathrm{elec}}+H_{\mathrm{solv}}+H_{\mathrm{bb}}. \tag{2.6}$$

In the second-quantized form, the electronic and solvent Hamiltonians are the same as in Schmickler's models,

$$H_{\mathrm{elec}}=\epsilon_a n_a+\sum_k \epsilon_k n_k+\sum_k [V_k(x)c_k^+ c_a+V_k^*(x)c_a^+ c_k], \tag{2.7}$$

where n_a is the occupation number operator of the antibonding orbital, with c_a^+ and c_a the corresponding creation and annihilation operators. The electronic states on the metal are labeled by the quantum number k; n_k, c_k^+, and c_k denote the corresponding occupation number, creation, and annihilation operators. The V_k are the corresponding matrix elements.

In considering the solvent and its interaction with the molecule we follow ideas familiar from electron transfer theory and distinguish between fast (electronic) and slow solvent modes. The former are assumed to be instantaneous and incorporated in the electronic energy ϵ_a. The slow solvent modes are represented as a collection of harmonic oscillators; their interaction with the molecule is assumed to be linear and proportional to the charge accumulated in the antibonding orbital. Thus H_{sol} reads

$$H_{\mathrm{sol}}=\frac{1}{2}\sum_\nu \hbar\omega_\nu(p_\nu^2+q_\nu^2)-n_a\sum_\nu \hbar\omega_\nu g_\nu(x)q_\nu. \tag{2.8}$$

The first term denotes the unperturbed solvent; q_ν and p_ν are the dimensionless coordinates and momenta, ω_ν the frequencies and ν labels the solvent modes. The second term accounts for the interaction. The $g_\nu(x)$ are the coupling constants. They depend on the distance x to account for a change in solvation as the molecule approaches the surface (see below).

The term H_{bb} describes the change in the potential energy of the bond as the antibonding orbital gets occupied by metal electrons. As in Savéant's model,[29] the $X-X$ bond is described by a Morse potential $[E_b(X_2)]$. In contrast to Savéant's model, we assume that by occupying the antibonding orbital with an electron, the bond weakens but the molecule does not break up. The breaking-up depends on how the energy of the molecule compares to the energy of the two adsorbed fragments. The molecular ion bond potential is also a Morse potential $[E_b(X_2^-)]$. By multiplying these potentials by the operators $[1-n_a]$ and n_a, we construct an effective switching function describing the weakening of the bond,

$$H_{bb}=[1-n_a]E_b(X_2)+n_a E_b(X_2^-). \tag{2.9}$$

The Morse potential for X_2 is

$$E_b(X_2)=D_e\{[1-\exp(-a(r-r_0))]^2-1\}, \tag{2.10}$$

where r is the bond distance, r_0 the equilibrium bond distance, and D_e the dissociation energy. The parameter a is related to the bond vibration frequency ω_b (in s^{-1}) by $a=\omega_b(\mu/2D_e)^{1/2}$, with μ the reduced mass of the atoms participating in the bond breaking process. For convenience, we choose a bond potential for X_2^- consisting of the same parameters, i.e.,

$$E_b(X_2^-)=D_e\{[1-\exp(-a(r-r_0))]^2 -1+\exp(-2a(r-r_0))\}. \tag{2.11}$$

The two potentials are drawn in Fig. 2. Note that, in this model, the dissociation energy for X_2^- is exactly half that of X_2, which is a reasonable estimate. For instance, our model predicts that for Cl_2^- the dissociation energy is 1.24 eV (1.30 eV experimentally), for Br_2^- 0.99 eV (1.15 eV experimentally), and I_2^- for 0.77 eV (1.0 eV experimentally).[31]

By well-known techniques detailed elsewhere,[7] one calculates for the ground-state PES $E_1(x,r,q)$,

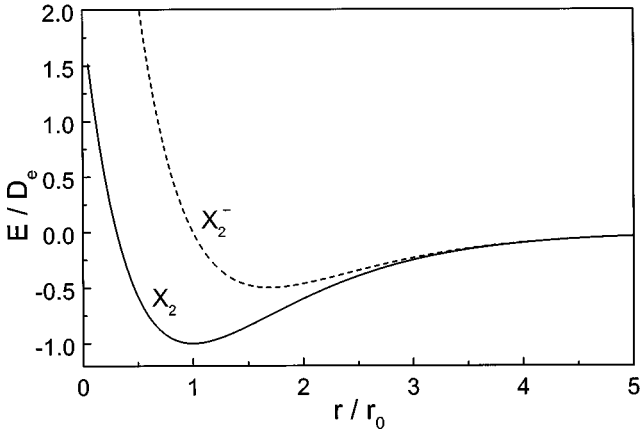

FIG. 2. The Morse bond potentials Eqs. (2.10) and (2.11).

$$E_1(x,r,q)=\tilde{\epsilon}_a(x,r,q)\langle n_a\rangle + \frac{\Delta_1(x)}{2\pi}\ln\frac{\tilde{\epsilon}_a^2(x,r,q)+\Delta_1^2(x)}{(\tilde{\epsilon}_a(x,r,q)-E_c)^2+\Delta_1^2(x)} + \lambda_1(x)q^2+E_b(X_2)+V_{X_2}(x) \tag{2.12}$$

with $\langle n_a(x,r,q)\rangle$ the average occupation of the antibonding orbital, given by

$$\langle n_a(x,r,q)\rangle=\frac{1}{\pi}\,\mathrm{arccot}\left(\frac{\tilde{\epsilon}_a(x,r,q)}{\Delta_1(x)}\right). \tag{2.13}$$

As equations very similar to Eqs. (2.12)–(2.13), including the detailed derivation, are given at many places in the literature,[7,8,9,13,17] we do not repeat their derivation here. Equation (2.12) is the exact solution of the ground-state PES of the above Hamiltonian if it is assumed that the width of the Fermi distribution of the metal electronic states can be neglected, and if the parameter Δ_1, which describes the electronic interaction of the diatomic with the surface, is independent of the electronic energy ϵ. The first term in Eq. (2.12) corresponds to the energy of the electron(s) occupying the antibonding orbital; the second term is the electronic bonding energy of the diatomic adsorbate, and equals zero at infinite distance from the surface where $\Delta_1=0$; the third term is (free) energy of solvation of the diatomic when it carries a charge $-q$; the fourth term is bonding energy of the diatomic; and the fifth term is the interaction of the core of the diatomic with the metal surface. A more detailed explanation and definition of the various quantities in Eq. (2.12) now follows.

(a) $\Delta_1(x)=\pi\Sigma_k|V_k(x)|^2\delta(\epsilon-\epsilon_k)$ is the broadening of the molecule's antibonding orbital energy, due to the electronic interaction with the metal states. Equation (2.12) can only be derived if Δ_1 is assumed that to be independent of the energy ϵ (wide conduction band approximation). Δ_1 falls off approximately exponentially with the distance of the molecule from the surface. We take $\Delta_1(x)=\Delta_1^0\exp(-x/l)$, with $l=1$ Å.

(b) $q=\Sigma_\nu q_\nu/g_\nu$ is the so-called generalized solvent coordinate familiar from the Marcus theory.[22] In Hush's interpretation,[27] $-q$ is equal to the (fractional) charge on the molecule.

(c) E_c is the energy of the bottom of the conduction band. Its exact value is immaterial; in all that follows we have taken it equal to -12 eV.

(d) The term $\tilde{\epsilon}_a(x,r,q)$ is the renormalized antibonding energy level, given by

$$\tilde{\epsilon}_a(x,r,q)=\epsilon_a+\Phi+\Delta\psi_{M/\mathrm{solv}}-2\lambda_1(x)q+E_b(X_2^-) - E_b(X_2)-\lambda_1^f(x)-\epsilon_{im}(x)+F(x)\Delta\phi. \tag{2.14}$$

(e) As mentioned, ϵ_a is the energy of the antibonding orbital, or the electron affinity of the X_2 molecule, $\epsilon_a=-EA(X_2)$.

(f) Φ is the work function of the metal; $\Delta\psi_{M/\mathrm{solv}}$ is the change in the surface dipole potential at the metal/solvent interface, due to changes in both the metal and solvent surface dipole potentials as a consequence of the presence of other phase. The quantity $\Phi+\Delta\psi_{M/\mathrm{solv}}$ may be viewed as the ''electrochemical work function,'' or as the potential of zero charge E_{pzc} on the vacuum or absolute scale.[32] This term is added to ϵ_a so that the Fermi level of the metal corresponds to the electronic energy zero.

(g) $\lambda_1(x)=\Sigma_\nu\hbar\omega_\nu g_\nu^2(x)/2$ is the distance dependent solvent reorganization energy. Its bulk value is estimated as the slow part of the molecular ion's real solvation energy, i.e., $\lambda_1(\infty)=-(\epsilon_{\mathrm{opt}}^{-1}-\epsilon_s^{-1})/(1-\epsilon_s^{-1})\times\Delta G_{\mathrm{solv}}^r(X_2^-)$. ϵ_{opt} and ϵ_s are the optical and static dielectric constants of the solvent, and for practically all solvents the quantity $(\epsilon_{\mathrm{opt}}^{-1}-\epsilon_s^{-1})/(1-\epsilon_s^{-1})\approx 0.5$. Experimental values for the molecular ion's real solvation energy are not available, but a rough guess can be made from the idea that an X_2^- is about twice as large as an X^-, which in the Born-model would lead to a $2^{1/3}$ smaller solvation energy. Molecular dynamics simulations show that the solvent's potential of mean force depends on the distance from the electrode surface; an ion has to overcome a solvent barrier in order to adsorb onto the metal.[33,34] One can take this important effect into account by introducing a distance-dependent solvation energy. We follow Schmickler's parameterization for the distance dependence;[17,20]

$$\lambda(x)=\lambda(\infty)[\xi+(1-\xi)p((x-r_a)/L)], \tag{2.15}$$

where ξ is the fraction of the bulk solvation energy that the ion experiences in the adsorbed state, and $p(x)$ is an interpolating function given by

$$\begin{aligned} &p(y)=0 \ \text{ for } \ y<0,\\ &p(y)=(3-2y)y^2 \ \text{ for } \ 0\leqslant y\leqslant 1,\\ &p(y)=1 \ \text{ for } \ y>1, \end{aligned} \tag{2.16}$$

r_a is the van der Waals radius of the atom, L is the distance at which λ reaches its bulk value, taken to be 4 Å.

(h) $\lambda_1^f(x)$ is the fast part of the distance-dependent solvation energy. Its bulk value is estimated as $\lambda_1^f(\infty) = -(1-\epsilon_{\rm opt}^{-1})/(1-\epsilon_s^{-1})\Delta G^r_{\rm solv}(X_2^-)$, its distance dependence has the same form as Eq. (2.16). Note that the sum of λ_1 and λ_1^f is simply the solvation energy of the monovalent ion.

(i) $\epsilon_{\rm im}(x)$ is the image interaction of the electron occupying the antibonding orbital on the X_2 molecule with the electrode. This quantity is one of the most difficult to estimate reliably. We have adopted a rather arbitrary model in which we take the classical form for the image interaction for distances larger than r_a, with a distance-dependent dielectric constant as specified in Refs. 17 and 18. For distances shorter than r_a, we want to avoid that the image interaction overrules all other interactions so we fix it at the constant value it has for $x=r_a$. There are of course many other choices possible, but none of them changes the qualitative conclusions of this work, as long as the image interaction is attractive (which is sometimes debated in the literature[35]). Note that in the employed definition $\epsilon_{\rm im}$ is a positive quantity.

(j) $F(x)\Delta\phi$ is the electrostatic potential in the electric double layer. $\Delta\phi=(\eta+E_{\rm eq}-E_{\rm pzc})$ is the electrode potential with respect to the potential of zero charge. $E_{\rm eq}$ is the equilibrium potential; η is the overpotential. $F(x)$ models the distribution of the potential in the double layer region. As a rough estimate we have assumed a linear drop of the potential between the metal surface and the outer Helmholtz plane which is at $x=r_a+L$.[17]

(k) $V_{X_2}(x)$ is the interaction potential of the bare X_2 molecule with the metal surface. It includes effects of the interaction of the HOMO orbital with the metal electronic levels, van der Waals attraction, Pauli repulsion, etc.[36] For simplicity we again assume a Morse potential,

$$V_{X_2}(x)=D_{X_2}\{[1-\exp(-a_{X_2}(x-r_c))]^2-1\}. \tag{2.17}$$

We could have chosen a more complicated potential, in order to include a barrier for X_2 adsorption as is sometimes found for the interaction of a diatomic with the metal/vacuum interface.[26] However, this barrier is normally low and therefore omitted in our model.

Using literature values for the various parameters, one can calculate the three-dimensional PES for the interaction of the molecule with the metal surface. To determine whether the molecule is stable with respect to the fragments, we need a more specific description of the interaction of the fragments with the metal. This is considered in the next subsection.

B. X^- adsorption

For the interaction of the X^- fragments with the metal surface, we employ Schmickler's model for electrochemical ion transfer.[17] Again, to keep matters simple, we treat the electron as spinless. This is certainly good enough for our conceptual purposes. The only interaction term that needs to be added with respect to Schmickler's model is the repulsion between the two fragments.

The expression for the ground-state PES is

$$\begin{aligned} E'(x,r,q) &= \tilde{\epsilon}_i(x,r,q_2)\langle n_i(x,r,q_2)\rangle \\ &\quad + \frac{\Delta_2(x)}{2\pi}\ln\frac{\tilde{\epsilon}_i^2(x,r,q_2)+\Delta_2^2(x)}{(\tilde{\epsilon}_i(x,r,q_2)-E_c)^2+\Delta_2^2(x)} \\ &\quad + \lambda_2(x)q_2^2 + V_X(x) + V_{X-X}(r) \end{aligned} \tag{2.18}$$

with $\langle n_i(x,r,q_2)\rangle$ the average occupation of the ion's orbital, given by

$$\langle n_i(x,r,q_2)\rangle = \frac{1}{\pi}\,\mathrm{arccot}\left(\frac{\tilde{\epsilon}_i(x,r,q_2)}{\Delta_2(x)}\right). \tag{2.19}$$

The various symbols and terms in Eq. (2.18) have the following meaning:

(i) $q_2=q/2$.

(ii) $\Delta_2(x)$ is the broadening of the ion's orbital energy. It has the same parameterization as $\Delta_1(x)$.

(iii) $\tilde{\epsilon}_i(x,r,q)$ is the renormalized energy level on the ion, given by

$$\begin{aligned} \tilde{\epsilon}_i(x,r,q_2) &= \epsilon_i+\Phi+\Delta\psi_{M/\rm solv}-2\lambda_2(x)q_2 \\ &\quad -\lambda_2^f(x)-\epsilon_{\rm im}(x)+F(x)\Delta\phi. \end{aligned} \tag{2.20}$$

(iv) ϵ_i is the energy level on the ion, or the electron affinity of the atom; $\epsilon_i=-EA(X)$.

(v) $\lambda_2(x)$ and $\lambda_2^f(x)$ have the same meaning and parameterization as the solvation parameters in the previous section, with the difference that they are estimated from the real solvation energies of the X^- ion, for which tabulations exist.

(vi) $V_X(x)$ is the interaction potential of the atom with the metal surface. It includes van der Waals and Pauli contributions, but no electronic (covalent) and electrostatic (image-type) contributions. These latter two interactions are contained in the model, i.e., in the Δ_2 and $\epsilon_{\rm im}$ terms. It is taken equal to the repulsive part of the Morse potential of Eq. (2.17).

(vii) $V_{X-X}(r)$ is the repulsion between two fragments. We take it equal to the repulsive part of the Morse potential in the previous section, i.e., $V_{X-X}(r)=D_e\times\exp(-2a(r-r_0))$. This is a rather severe approximation, as in a more consistent treatment it should more explicitly treat electrostatic and covalent contributions, which both depend on the electron occupation of the fragments.

(viii) All the other symbols have the same meaning as in the previous section.

The potential energy surface for comparison with that of the molecule must be that of two fragments, correcting for the double counting of their interaction. Hence,

$$E_2(x,r,q)=2E'(x,r,q)-V_{X-X}(r). \tag{2.21}$$

C. The total potential energy surface

In calculating the PES of the total reaction, we follow a suggestion made by Harris[37] and Darling and Holloway[38] for the dissociative adsorption of diatomics at the metal/vacuum interface. We couple the E_1 and E_2 PES through the mixing parameter $V_{12}(x,r)$. The total PES then simply follows from

$$E_{\mathrm{tot}}(x,r,q)=\frac{E_1(x,r,q)+E_2(x,r,q/2)-[(E_1(x,r,q)-E_2(x,r,q/2))^2-4(V_{12}(x,r))^2]^{1/2}}{2}. \tag{2.22}$$

As we have no good way to estimate V_{12} we usually take it as small, such that Eq. (2.22) essentially reduces to taking the lowest energy of the two. The interaction element is assumed to fall off exponentially with x and r, $V_{12}(x,r)=V_{12}^0\exp(-x/l_x)\exp(-r/l_r)$, with l_x and l_r both taken at 1 Å. Although this approach does not have a rigorous quantum-mechanical basis, it should provide a plausible ansatz for interpolating between the two PES.

Before we study in detail the shape of the PES and the predictions it makes about activation energies, transfer coefficients, etc., let us perform a small check that our parameterization is indeed correct. Putting the overpotential $\eta=0$, and equating $E_1(x=\infty,\ r=r_0,\ q=0)$ and $E_2(x=\infty,\ r=\infty,\ q_2=1)$, we should obtain an expression for E_{eq} in terms of the various thermodynamic quantities. We get the Born–Haber expression,

$$E_{\mathrm{eq}}=-\Delta G^r_{\mathrm{solv}}(X^-)+EA(X)-0.5D_e-(\Phi+\Delta\psi_{M/\mathrm{solv}}-E_{\mathrm{pzc}}), \tag{2.23}$$

which is simply the ''work function'' for the $X_2+2e^-\rightleftharpoons 2X^-$ reaction[25] minus a constant which relates the vacuum scale to the electrochemical scale to which we choose to refer E_{pzc} and E_{eq} (note that, on the vacuum scale, $E_{\mathrm{pzc}}=\Phi+\Delta\psi_{M/\mathrm{solv}}$). A common (though debated) value for this constant is 4.44 eV with respect to the NHE.[32] In Table I we give the various parameters for the chlorine, bromine, and iodine reduction and compare the calculated standard equilibrium potential with the experimental standard potentials.

TABLE I. Calculated and experimental standard potentials of $X_2+2e^-\rightleftharpoons 2X^-$ vs NHE (data from Refs. 31, 39, 40).

X	$\Delta G^r_{\mathrm{solv}}(X^-)$	EA(X)	$D_e(X_2)$	$E^{\mathrm{calc}}_{\mathrm{eq}}$ [Eq. (2.23)]	$E^{\mathrm{ex}}_{\mathrm{eq}}$
Cl	−3.29	3.613	2.479	1.224	1.358
Br	−3.15	3.363	1.970	1.088	1.087
I	−2.67	3.063	1.542	0.522	0.535

D. The $Y_2/2Y$ PES

The PES for reaction (2.2) is calculated from a very similar model to that presented in the previous sections. However, a few parameters and equations change, as explained subsequently.

For the interaction of the molecule with the electrode, we have

$$E_1(x,r,q)=\tilde{\epsilon}_a(x,r,q)\langle n_a\rangle+\frac{\Delta_1(x)}{2\pi}\ln\frac{\tilde{\epsilon}_a^2(x,r,q)+\Delta_1^2(x)}{(\tilde{\epsilon}_a(x,r,q)-E_c)^2+\Delta_1^2(x)}+\lambda_1(x)q^2+2z\lambda_1(x)q-z^2\lambda_1^f(x)-z^2\epsilon_{\mathrm{im}}(x)-zF(x)\Delta\phi+E_b(Y_2^+)+V_{Y_2}(x)+\mathrm{IP}(Y_2)-\Phi-\Delta\psi_{M/\mathrm{solv}}, \tag{2.24}$$

where $z=1$ is the charge of the Y_2^+ molecular ion. The last three terms are added to make the energy of the Y_2 molecule equal to $E_b(Y_2)$. The electronic energy level $\tilde{\epsilon}_a$ is given by

$$\tilde{\epsilon}_a=-\mathrm{IP}(Y_2)+\Phi+\Delta\psi_{M/\mathrm{solv}}-2\lambda_1(x)q+F(x)\Delta\phi+E_b(Y_2)-E_b(Y_2^+)+\lambda_1^f(x)+\epsilon_{\mathrm{im}}(x) \tag{2.25}$$

and is related to the average occupation of the orbital $\langle n_a\rangle$ by Eq. (2.13). IP(Y_2) is the ionization potential of the Y_2 molecule. The bond potentials are given by

$$E_b(Y_2)=D_e\{[1-\exp(-a(r-r_0))]^2-1\} \tag{2.26}$$

and

$$E_b(Y_2^+)=D_e\{[1-\exp(-a(r-r_0))]^2-1+\exp(-2a(r-r_0))\}. \tag{2.27}$$

The energy of a fragment is

$$E'(x,r,q_2)=\tilde{\epsilon}_i(x,r,q_2)\langle n_i(x,r,q_2)\rangle+\frac{\Delta_2(x)}{2\pi}\ln\frac{\tilde{\epsilon}_i^2(x,r,q_2)+\Delta_2^2(x)}{(\tilde{\epsilon}_i(x,r,q_2)-E_c)^2+\Delta_2^2(x)}+\lambda_2(x)q_2^2+2z\lambda_2(x)q_2-z^2\lambda_2^f(x)-z^2\epsilon_{\mathrm{im}}(x)-zF(x)\Delta\phi+V_Y(x)+V_{Y-Y}(r)+\mathrm{IP}(Y)-\Phi-\Delta\psi_{M/\mathrm{solv}} \tag{2.28}$$

with

$$\tilde{\epsilon}_i=-\mathrm{IP}(Y)+\Phi+\Delta\psi_{M/\mathrm{solv}}+F(x)\Delta\phi-2\lambda_1(x)q_2+\lambda_f(x)+\epsilon_{\mathrm{im}}(x), \tag{2.29}$$

where IP(Y) is the ionization potential of the Y atom. The total energy of the two fragments is calculated as before [Eq. (2.21)]. The equilibrium potential E_{eq} is given by

$$E_{\mathrm{eq}}=\Delta G^r_{\mathrm{solv}}(Y^+)+\mathrm{IP}(Y)+0.5D_e-(\Phi+\Delta\psi_{M/\mathrm{solv}}-E_{\mathrm{pzc}}). \tag{2.30}$$

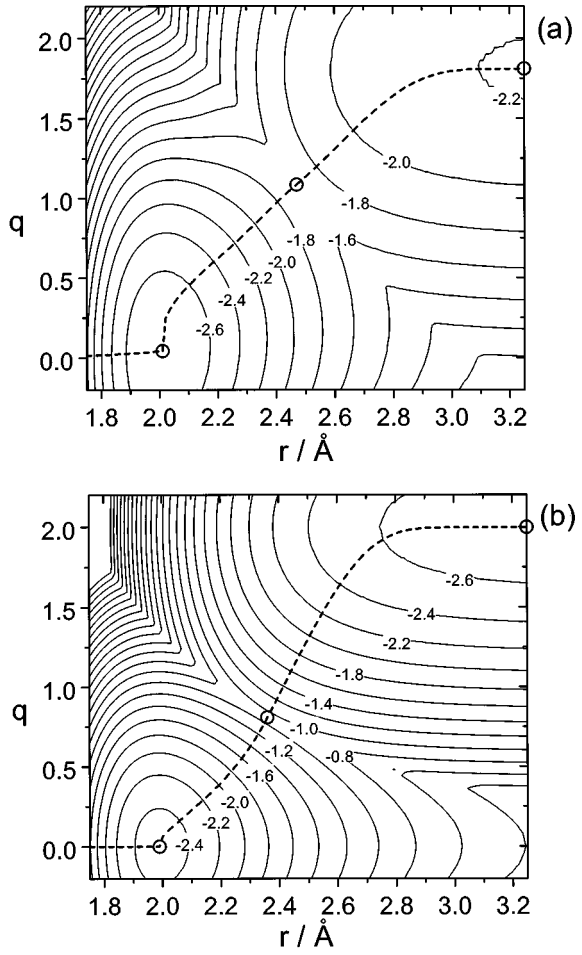

FIG. 3. (a) Contour plot in the $r-q$ plane of the PES for $X_2+2e^- \rightleftharpoons 2X^-$ at $x=1.8$ Å. (b) As in (a) but for $x=6.0$ Å. Parameters, $\Delta G^r_{\mathrm{solv}}(X^-)=3.29$ eV, $\Delta G^r_{\mathrm{solv}}(X_2^-)=2.61$ eV, $\epsilon_\infty=1.85$, $\epsilon_s=78.6$, $\mathrm{EA}(X)=3.11$ eV, $\mathrm{EA}(X_2)=2.15$ eV, $\Phi+\Delta\psi_{M/\mathrm{solv}}=E_{\mathrm{pzc}}=4.3$ eV, $\Delta_1^0=3$ eV, $\Delta_2^0=3$ eV, $r_c=1.81$ Å, $L=4$ Å, $D_e=2.479$ eV, $r_0=1.988$ Å, $a=1.977$ Å^{-1}, $\xi=0.5$, $V_{12}^0=0.1$ eV, $D_{X_2}=0.2$ eV, $a_{X_2}=2.5$ Å^{-1}.

III. PROPERTIES OF THE PES

As our PES are three-dimensional, we have to devise a method to picture them in a convenient and physically meaningful way. To this end, we calculate the PES in the $r-q$ plane by constraining the distance x from the surface at a series of values. Two examples of a PES contour plot at a distance close (1.8 Å) and a distance further away (6 Å) from the surface are shown in Figs. 3(a) and 3(b). In these figures, we have chosen values for the various parameters that should approximately apply to the chlorine/chloride reaction, which are given in the figures' captions. (The parameters Δ_1^0, Δ_2^0, V_{12}^0, and ξ should come from quantum-chemical and molecular dynamics calculations and have been given reasonable and hopefully realistic values.) On these two-dimensional PES the steepest-descent path is calculated from the one minimum [characteristic of the (adsorbed) X_2] through a saddle point to the other minimum [characteristic of two (adsorbed) X^-]. Of course, the latter minimum really lies at infinite separation r, but for convenience it is cut off at (the arbitrary value of) 3.25 Å. These paths are shown as the dashed lines in the contour plots. For separations smaller than r_0, the dashed line shows the minimum energy. From the one-dimensional reaction paths calculated at various x in the $r-q$ plane, the ''full'' PES in Fig. 4 is constructed. The contour plot of Fig. 4 is shown in Fig. 5, where the dashed line is again the reaction path. These surfaces clearly illustrate the principle of catalysis; close to the electrode surface, the activation energy to dissociation is significantly reduced with respect to, say, the outer Helmholtz plane. It is important to realize that to every point on the PES of Fig. 4 there belongs a different value of q. In Fig. 6 it is shown how the energy and the solvent coordinate q change along the reaction path. The reaction coordinate here is a mixture of r and x. During the actual breaking up of the molecule, the system mainly moves along the r-coordinate, as can be seen from the reaction path in Fig. 4. During the desorption of the two fragments, the system moves along the x-coordinate: this process is of course Schmickler's ion transfer.[17]

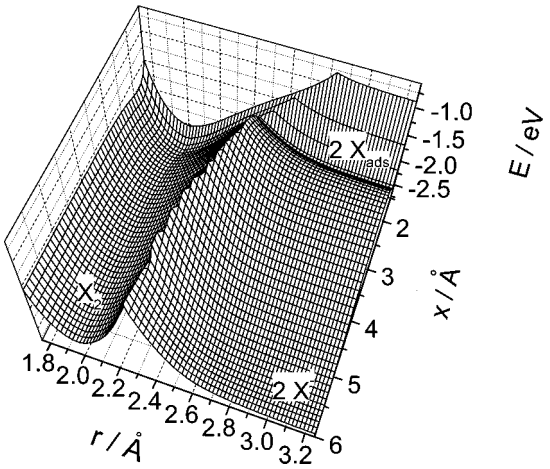

FIG. 4. Total PES at equilibrium in the $r-x$ plane as explained in the text. Parameters as in Fig. 3.

A very similar PES is calculated for reaction Eq. (2.2). A typical example is shown in Fig. 7. The parameters here do not reflect any reaction in particular, as we want avoid giving the impression that this is a reasonable model for the hydrogen oxidation.

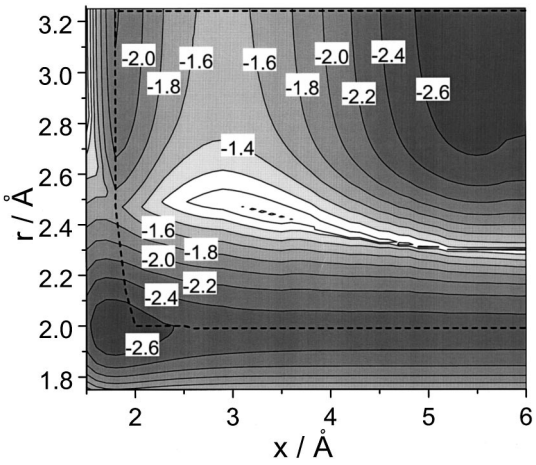

FIG. 5. Contour plot of Fig. 4. Dashed line is the reaction path.

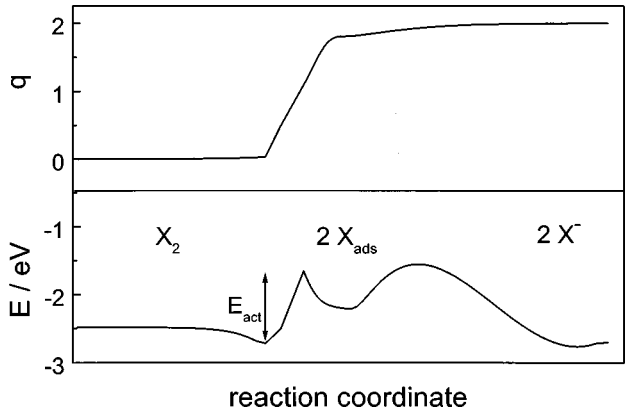

FIG. 6. The energy E and the solvent coordinate q along the reaction path drawn in Fig. 5.

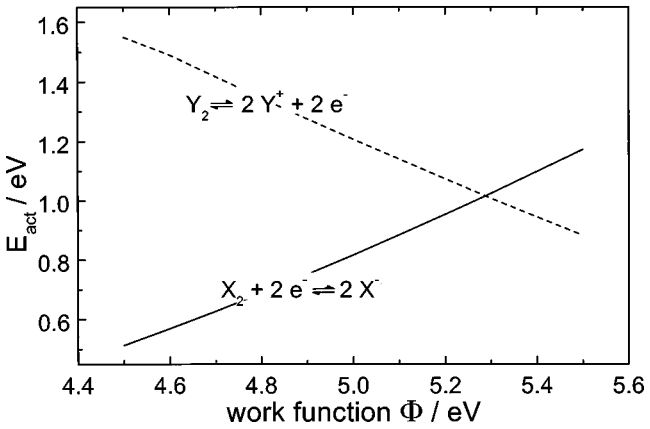

FIG. 8. Work function dependence of the activation energy E_{act} as defined in Fig. 6. $\Delta\psi_{M/\mathrm{solv}}=0.7$ eV. Other parameters as in Figs. 3 and 7.

According to classical transition state theory, the rate of the reaction will depend on the energy of the saddle point of the PES, which is the transition state or the activated complex for the reaction. There are two such transition states in our model, in agreement with the idea that the reaction takes place in two steps, and the most interesting for our purposes is the activation energy to dissociative adsorption, as defined in Fig. 6. It is of interest to calculate this energy as a function of the work function of the metal catalyst, as this experimental parameter does not affect the overall thermodynamics of the reaction. In Fig. 8 we show how the activation energy at equilibrium changes with the work function of the substrate. Opposite trends are observed for the oxidative and reductive dissociative adsorption. For reaction (2.1) the activation energy decreases with decreasing work function; for reaction (2.2) the activation energy increases with decreasing work function. The latter trend has indeed been extracted from the literature data by Trassati for the $H_2 \rightleftharpoons 2H^+ + 2e^-$ reaction.[32]

It is interesting to analyze the physical origin of this trend (in our model) and the meaning of the slope of the curves shown in Fig. 8. First, we find that the change in the energy of the transition state is directly related to a change in the adsorption energy of the fragment with the work function. If we consider reaction (2.1), the adsorption energy of the X fragment gets more negative with decreasing work function. For the parameter values in Fig. 8, the slope of this curve is ~ 0.65. The value is exactly the electrosorption valency $-\gamma_X$ of X. In our model, the electrosorption valency would be equal to $\gamma = zg - \zeta(1-g)$, where z is the valency of the (bulk) ion, ζ is the partial charge transferred from the adsorbed ion to the metal, and g is a geometrical factor which expresses the fraction of the double layer potential that is actually experienced by the adsorbed ion.[25] For the data in Fig. 8, $z=-1$, $g \approx 0.69$, $\zeta \approx -0.1$, which indeed agrees with the slope of the curve. The activation energy for dissociation changes with the adsorption energy of the fragments following a Brønsted relationship,

$$\frac{dE_{\mathrm{act}}}{2dE_{\mathrm{ads}}} = \alpha_B , \tag{3.1}$$

where α_B is the Brønsted coefficient for dissociation. Hence, for the work function dependence of reaction (2.1), we find

$$\frac{dE_{\mathrm{act}}}{d\Phi} = -2\gamma_X \alpha_B . \tag{3.2}$$

From Fig. 8, we find that $dE_{\mathrm{act}}/d\Phi = 0.66$ and hence $\alpha_B \approx 0.51$, which is close to the expected value of 1/2. For a plot of $d \ln i_0/d\Phi$, where i_0 is the exchange current density at equilibrium, this would imply a slope of 25.5 eV^{-1} (for the hydrogen couple, Trasatti's data[32] give a slope of $\sim 16\ \mathrm{eV}^{-1}$).

The potential dependence of the activation energy, for one typical value of the work function, is shown in Fig. 9. As expected, it decreases with more negative overpotential. Again, there is a one-to-one correspondence with the adsorption energy of the fragment. The adsorption energy of the X fragment gets more positive with more negative overpotential. However, the adsorption energy is referred to the X^- state in the bulk, whereas the reaction energy of the dissociation step is referred to the $X_2 + 2e^-$ state. Therefore, for the slope of Fig. 9, we find

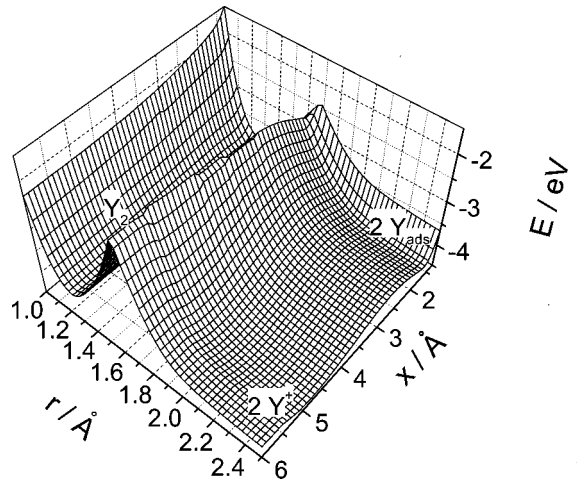

FIG. 7. PES in the $r-x$ plane for the $Y_2 \rightleftharpoons 2Y^+ + 2e^-$ reaction at equilibrium. Parameters, $\Delta G^r_{\mathrm{solv}}(Y^+) = 4$ eV, $\Delta G^r_{\mathrm{solv}}(Y_2^+) = 3$ eV, $\epsilon_\infty = 1.85$, $\epsilon_s = 78.6$, $\mathrm{IP}(Y) = 5$ eV, $\mathrm{IP}(Y_2) = 7$ eV, $\Phi + \Delta\psi_{M/\mathrm{solv}} = E_{\mathrm{pzc}} = 4.3$ eV, $\Delta_1^0 = 3$ eV, $\Delta_2^0 = 3$ eV, $r_c = 1.5$ Å, $L = 4$ Å, $D_e = 4$ eV, $r_0 = 1.25$ Å, $a = 2$ $\mathrm{Å}^{-1}$, $\xi = 0.7$, $V_{12}^0 = 0.1$ eV, $D_{X_2} = 0.2$ eV, $a_{X_2} = 2.5$ $\mathrm{Å}^{-1}$.

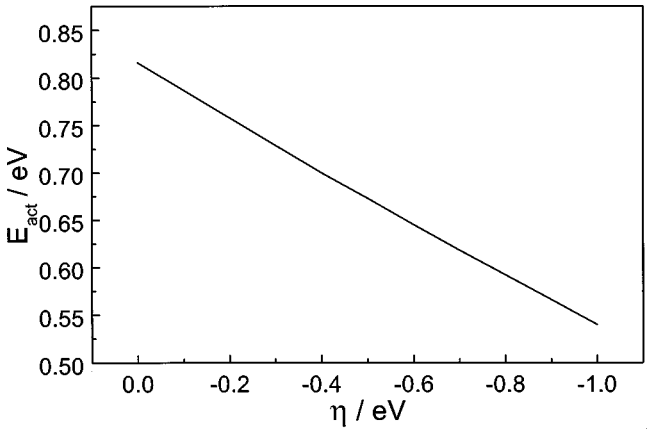

FIG. 9. Potential dependence of the activation energy for the electrocatalytic X_2 dissociation. $\Delta\psi_{M/\mathrm{solv}}=0.7$ eV. Other parameters as in Fig. 3.

$$\frac{dE_{\mathrm{act}}}{d\eta}=2(1+\gamma_X)\alpha_B. \tag{3.3}$$

(Recall that $\gamma_X<0$.) Note that the transfer coefficient, i.e., the slope $dE_{\mathrm{act}}/d\eta$, is significantly smaller than $\frac{1}{2}$, even though the Brønsted coefficient of the dissociation step proper is close to $\frac{1}{2}$. This is mainly due to the fact that at the adsorption site, the fragments feel only part of the total double layer potential, due to the geometrical g factor in the formula for the electrosorption valency. In the particular case of Fig. 9, the Butler–Volmer transfer coefficient is ~ 0.28. A consequence of formula (3.3) is that if $\gamma_X=-1$, the activation energy for dissociative adsorption (Tafel reaction) does not depend on the potential. This is, within the context of our model, a logical result as the X is completely discharged for $\gamma_X=-1$ and hence the dissociation is not accompanied by any electron exchange with the metal substrate; it is a purely heterogeneous chemical reaction. Of course, the ion transfer process (Volmer reaction) will depend markedly on the potential.[17,19]

Note that in the above analysis, we looked only at the activation energy of dissociation. In the overall reaction rate, the desorption of the fragment (ion transfer) also plays a role. The rate of this step shows the opposite dependence on the adsorption energy, and the combination of these two opposing trends for dissociation and subsequent desorption leads to the well-known volcano relationship.[26,32]

In our calculation, we find that the X_{ads} intermediate still carries a partial charge. Hence, a more general way to present the Tafel–Volmer mechanism is

$$\begin{aligned} &X_2+2\,\delta e^- \rightleftharpoons 2X_{\mathrm{ads}}^{\delta-},\\ &X_{\mathrm{ads}}^{\delta-}+(1-\delta)e^- \rightleftharpoons X^-. \end{aligned} \tag{3.4}$$

In our calculation above, δ is quite close to 1, but clearly this value depends on many factors, primarily on the electron affinity of X, the solvation energy of X^-, and the strength of the electronic interaction. More importantly, it will depend on the prevailing coverage of X_{ads}, and is expected to get closer to zero the higher the coverage.[5] Secondly, the distribution of the X_{ads} on the surface will depend on the lateral interactions and this will also exert an influence on the macroscopic rate.[41] Also note that in the above mechanism the partial charge $\delta(=1-\zeta)$ appears, but that in the experimental trends with potential or work function the electrosorption valency γ_X is the relevant quantity, as this quantity also includes the effect of the double layer.

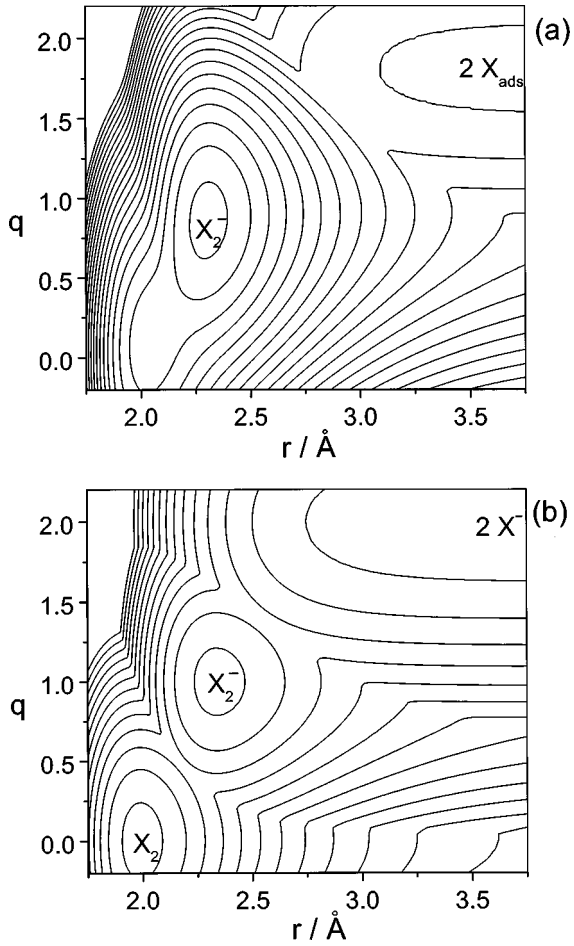

FIG. 10. Two contour plots at overall equilibrium in the $r-q$ plane for $\mathrm{EA}(X_2)=3.65$ eV. (a) $x=1.8$ Å, (b) $x=6$ Å. Other parameters as in Fig. 3.

Figures 3–6 apply to a relatively low or even negative electron affinity of the X_2 molecule. This parameter does usually not have a very significant effect on the activation energy of the dissociation. If the electron affinity is decreased by 2 eV, the activation energy increases (as expected) by ~ 0.1 eV for the values of the work function in Fig. 8. However, with increasing electron affinity of the molecule, a new minimum is formed at $q\approx 1$, and this leads to a qualitatively new and interesting picture. In Fig. 10 we show two contour plots of the PES close to the surface [1.8 Å, Fig. 10(a)] and far from the surface [6 Å, Fig. 10(b)], as in Fig. 3, but now for relatively high electron affinity. In the bulk of the solution, far from the surface, there is a new metastable minimum, corresponding to the X_2^- ion, which is stabilized by its high affinity to accept an electron, in conjunction with the gain in solvation energy. However, the direct transition from the X_2^- ion to two X^- ions is very unlikely at this distance, because the coupling constant V_{12}^0 should be very small here and hence the reaction is strongly nonadiabatic.

As the electrode surface is approached, the X_2^- is further stabilized by the image interaction, provided it counterbalances for the loss in solvation energy. Therefore close to the surface [Fig. 10(a)] only one minimum remains, corresponding to the X_2^- ion. Clearly, our model is by far not accurate enough to make quantitative predictions, but it seems that the qualitative conclusion is justified that under these circumstances, a variant of the Tafel–Volmer mechanism may apply, namely,

$$\begin{aligned} &X_2+\beta e^- \rightleftharpoons X_{2,\mathrm{ads}}^{\beta-}, \\ &X_{2,\mathrm{ads}}^{\beta-}+(2\delta-\beta)e^- \rightleftharpoons 2X_{\mathrm{ads}}^{\delta-}, \\ &X_{\mathrm{ads}}^{\delta-}+(1-\delta)e^- \rightleftharpoons X^-, \end{aligned} \tag{3.5}$$

where $\beta \approx 1$.

IV. SUMMARY AND CONCLUSION

In this paper, we have presented a simple model for dissociative adsorption and associative desorption at metal electrodes. Our model allows the calculation of the PES of these reactions, assuming that they follow a Volmer–Tafel mechanism. We have studied and rationalized the trends in the activation energy with changing the work function of the metal (at equilibrium), and with the electrode potential of the metal (driving the system away from equilibrium). We found that the activation energy for dissociation is closely related to the adsorption energy of the fragment. Two important parameters in the observed trends, which also determine the Butler–Volmer transfer coefficient, are the Brønsted coefficient of the dissociation step proper (which is about 1/2) and the electrosorption valency of the adsorbed fragment. Two key quantities in the electrosorption valency are the location of the fragment in the electric double layer, i.e., how much of the total double layer potential is actually felt by the adsorbed species, and the partial charge transferred from the fragment to the metal electrode. We have shown that in our model, the activation energy is less sensitive to the changes in the energy of the antibonding or bonding orbital responsible for the breaking-up of the molecule. However, for extreme values of the orbital energies, molecular ions may become metastable and affect the overall reaction mechanism.

An important simplification in our treatment is that we have neglected electron spin and that we did not account correctly for the interaction between the two fragments. Clearly the mixing of the two PES by Eq. (2.22), though circumventing a significant increase in complexity, is not very satisfactory from the quantum-mechanical point-of-view. The main advantage of our approach is that the PES is easily calculated in many dimensions, allowing us to obtain a illustrative and pictorial view on catalytic bond breaking at metal electrodes. The drawbacks of our model could (and should) be remedied by resorting to a single Hamiltonian model, and we intend to explore this in future work. However, this will require the specification of several orbital levels, the inclusion of electron spin, and hence a much more time-consuming self-consistent numerical solution of the PES. Furthermore, we do not expect such improvements to modify significantly the qualitative trends extracted from the simpler approach adopted in this paper. More substantial progress can also be expected from detailed molecular dynamics simulations of two ions interacting with the metal, the solvent, and each other. Such results may also shed light on how to decide whether a given reaction follows a Volmer–Tafel or Volmer–Heyrovsky mechanism. This is definitely a next important step in understanding electrocatalytic bond breaking and bond formation at the metal/liquid interface.

ACKNOWLEDGMENTS

The research of M.T.M.K. was made possible by a fellowship from the Royal Netherlands Academy of Arts and Sciences (KNAW). G.A.V. was supported by a grant from the United States Office of Naval Research. We also thank Professors Rutger van Santen and Wolfgang Schmickler for their comments on the manuscript.

[1] R. A. van Santen and M. Neurock, Catal. Rev. Sci. Eng. **37**, 357 (1995).
[2] A. B. Anderson, J. Electroanal. Chem. **280**, 37 (1990).
[3] A. B. Anderson, R. W. Grimes, and S. Y. Hong, J. Phys. Chem. **91**, 4245 (1987).
[4] W. Schmickler, J. Electroanal. Chem. **100**, 533 (1979).
[5] A. A. Kornyshev and W. Schmickler, J. Electroanal. Chem. **185**, 253 (1985).
[6] P. W. Anderson, Phys. Rev. **124**, 41 (1961); D. M. Newns, *ibid.* **178**, 1123 (1969).
[7] W. Schmickler, J. Electroanal. Chem. **209**, 31 (1986).
[8] K. L. Sebastian, J. Chem. Phys. **90**, 5056 (1989).
[9] B. B. Smith and J. T. Hynes, J. Chem. Phys. **99**, 6517 (1991).
[10] J. B. Straus, A. Calhoun, and G. A. Voth, J. Chem. Phys. **102**, 529 (1995).
[11] A. Calhoun and G. A. Voth, J. Phys. Chem. **100**, 10746 (1996).
[12] M. T. M. Koper, J.-H. Mohr, and W. Schmickler, Chem. Phys. **230**, 95 (1997).
[13] Y. Boroda, A. Calhoun, and G. A. Voth, J. Chem. Phys. **107**, 8940 (1997).
[14] Y. Boroda and G. A. Voth, J. Chem. Phys. **104**, 6188 (1996).
[15] B. B. Smith and A. J. Nozik, Chem. Phys. **205**, 47 (1996).
[16] A. M. Kuznetsov, J. Electroanal. Chem. **159**, 241 (1983).
[17] W. Schmickler, Chem. Phys. Lett. **237**, 152 (1995).
[18] W. Schmickler, Electrochim. Acta **41**, 2329 (1996).
[19] M. T. M. Koper and W. Schmickler, Chem. Phys. **211**, 123 (1996).
[20] M. T. M. Koper and W. Schmickler, J. Electroanal. Chem. (in press).
[21] M. T. M. Koper and G. A. Voth, Chem. Phys. Lett. **282**, 100 (1998).
[22] R. A. Marcus, J. Chem. Phys. **24**, 966 (1956); **43**, 679 (1965).
[23] V. G. Levich, in *Physical Chemistry, An Advanced Treatise*, edited by H. Eyring, D. Henderson, and W. Jost (Academic, New York, 1970), Vol. 9b, p. 986; R. R. Dogonadze, in *Reactions of Molecules at Electrodes*, edited by N. S. Hush (Wiley, New York, 1971), p. 135.
[24] K. J. Vetter, *Electrochemical Kinetics* (Academic, New York, 1967).
[25] W. Schmickler, *Interfacial Electrochemistry* (Oxford University Press, New York, 1996).
[26] R. A. van Santen and J. W. Niemantsverdriet, *Chemical Kinetics and Catalysis* (Plenum, New York, 1995).
[27] N. S. Hush, J. Chem. Phys. **28**, 962 (1958).
[28] R. A. van Santen, *Theoretical Heterogeneous Catalysis* (World Scientific, Singapore, 1991).
[29] J.-M. Savéant, J. Am. Chem. Soc. **109**, 6788 (1987); Acc. Chem. Res. **26**, 455 (1993).
[30] S. Holloway and J. K. Nørskov, J. Electroanal. Chem. **161**, 193 (1984).
[31] A. A. Radzig and B. M. Smirnov, *Reference Data on Atoms, Molecules and Ions*, Springer Series in Chemical Physics (Springer, Berlin, 1985), Vol. 31.
[32] S. Trasatti, in *Advances in Electrochemistry and Electrochemical Engineering*, edited by H. Gerischer and C. W. Tobias (Wiley Interscience, New York, 1977), Vol. 10, p. 213.
[33] E. Spohr, Chem. Phys. Lett. **207**, 214 (1993).

[34] O. Pecina, E. Spohr, and W. Schmickler, J. Electroanal. Chem. **394**, 29 (1995).
[35] P. Dzhavakhidze, A. A. Kornyshev, and L. I. Krishtalik, J. Electroanal. Chem. **228**, 329 (1987).
[36] J. Harris, S. Andersson, C. Holmberg, and P. Nordlander, Phys. Scr. **T13**, 155 (1986).
[37] J. Harris, Surf. Sci. **221**, 335 (1989).
[38] G. R. Darling and S. Holloway, Rep. Prog. Phys. **58**, 1595 (1995).
[39] *Standard Potentials in Aqueous Solution*, edited by A. J. Bard, R. Parsons, and J. Jordan (Marcel Dekker, New York, 1985).
[40] *American Institute of Physics Handbook*, edited by D. E. Gray (McGraw–Hill, New York, 1972).
[41] M. T. M. Koper, Electrochim. Acta (in press).